Nanotubes – an Outstanding Set of Nano Particles?

Reinhard Nesper* and Hans-Joachim Muhr

Abstract. Nano particles constitute a fascinating class of material which is still difficult to access. Modern developments in chemical syntheses, like template- and tenside-aided reactions, downscaling of physical lithography, and availability of high-resolution microscopy, like the scanning probe and electron microscopy, have opened doors into this size regime. The nanotube materials seem to be most attractive because of their large anisotropy and geometrical pre-functionalization. More and more routes towards nanotube materials are being explored based on quite different chemical compounds. Different growth mechanisms are discussed, the study and control of which is a key point of generating well-defined nanotubes. These may serve as hosts for future nano devices.

1. Introduction

'Size is everything' is the title of a recent comment of *R.S. Berry* [1] referring to the observation of the coexistence of 'solid and liquid clusters' in sodium nano particles by *Schmidt et al.* [2]. It may not be all, but it is very important for any type of matter and this importance increases rapidly by reaching nano dimensions. The design of nanoscopic entities is an ongoing task on a way of which only the first steps have been taken, hitherto. Most important for the future of science, technology, and applications is that developments in nano science strongly demand interdisciplinary cooperation because neither chemical nor physical nor technological approaches are powerful enough to enter this field successfully on their own. Achievements in nanotechnology will necessarily demand for transdisciplinary creativity and expertise which will be a matter of R&D groups of individuals of quite different education but open minds for interaction.

Nano particles are extremely attractive because of several reasons:

1) They belong to the size regime nature used for building its enormously effective biological devices;
2) They may allow for a linear downscaling of present technological devices by at least two orders of magnitude;
3) The amount of material – environmentally dangerous or not – for constructing devices may considerably be reduced giving rise to changed judgements in society about which compounds may be dangerous and which not;
4) The chemical activity of such particles is by orders of magnitude enhanced compared to macroscopic materials of the same chemical compositions;
5) The shape may become an intimate trigger for the functionality;
6) The physical properties change drastically giving rise to possible completely novel behavior like, *e.g.*, low-dimensional cooperative effects (*e.g.*, magnetic ordering, dipole ordering, ordinary and superconductivity);
7) Understanding of synthesis and functionality of nanoscopic entities will send fruitful impulses into many other research fields like *e.g.*, heterogeneous catalysis and materials research.

Correspondence: Prof. Dr. R. Nesper
Laboratorium für Anorganische Chemie
ETH-Zürich
Universitätstrasse 6
CH–8092 Zürich
Tel.: +41 1 632 30 69, Fax: +41 1 632 11 49
E-Mail: nesper@inorg.chem.ethz.ch

2. Nano Particles

However, reports of nano particles have a long history, a real tayloring of nanoscopic entities is by no means straightforward, and only very few examples are known which obey the conditions of sharp determination of shape and size, today. Although, the latter are well-developed for molecular systems on the one hand and microtechnology on the other, they are under enforced investigation in solid-state and biomineralization sciences. Closing this open gap is one of the prominent, fascinating goals of the research on nano particles.

The size domain we are talking about reaches from, say, two nanometers to one hundred nanometers, and, as already mentioned, shape will play an important role. We will give a short summary of distinct forms of such particles by which specific functionalities may be achieved starting with finite entities.

2.1. *Zero-Dimensional Nano Particles*

Spheroids are compact or hollow entities of more of less spherical form (*cf. Fig. 1, a–d*). Fullerenes are very prominent representatives of this class [3]. Because of their high uniformity, they may serve for very isotropic functions.

Tori constitute a different family to which large ring-shaped molecules belong (*Fig. 1, e* and *f*). Very beautiful examples of these have been synthesized in different fields of chemistry [4][5].

Mushroom- or umbrella-shaped entities carry a strong shape anisotropy which may be used to generate highly nonlinear effects (*Fig. 1, g* and *h* [6]).

Short rods or tubes with (*Fig. 1, k* and *l*) or without open ends (*Fig. 1, m* and *n*) can be thought of as extentions of plate-like or torus-shaped entities, by stack or growth processes (*Fig. 1, i–u* and *Fig. 2*).

A nearly infinite number of **motives of lower shape symmetry** is possible which, in the end, may be of such a specific type for that they constitute highly selective key-lock couples. Many of the large molecules which are used in supramolecular chemistry are part of this class.

All the previously mentioned categories may contain quasi-rigid entities (*Fig. 1, a, c, e, g, k, m*) or open grown-like species (*Fig. 1, b, d, f, h, j, l, n*) for which the class of **dendrimers** sets up excellent examples. The latter may be seen as a collective of (functional) species fused together or bound to a surface of another moiety to a higher hierarchical assembly to form complex nano particles.

2.2. *One-Dimensional Nano Particles*

The 1D representatives we would like to mention here, may have one macroscopic dimension (*e.g.*, in the micron range) but are in the other two directions of nano

size. If suitable growth processes are found (*cf. Fig. 2*), some of the 0D entities may be transformed into 1D species.

Chains set up basic moieties for the wast field of polymer chemistry (*Fig. 1, o* and *p*). Although polymers are extremely well-handled in polymer science and technology, it is still a major problem to separate and align single chains; this problem is not solved in general terms for all other nano particles, as well.

Sheets are very anisotropically cut parts of 2D layered materials which have only strong interactions in two directions (*Fig. 1, t*). In case one dimension of the layer is very small, a narrow sheet is formed (of a few nanometers, depending on the type of compound and on its structure). If the dangling bonds at the borders can be saturated by some way, the sheet may be relatively stable, if not the relatively large number of dangling bonds along the long layer direction may be saturated by folding into a cylinder or a scroll.

Rods are more or less compact 1D entities, to which unbranched polymers belong (*Fig. 1, o*). These may be classical organic or inorganic polymers, but also metal, semiconductor or insulator wires like those which have already been generated inside of hollow nanotubes of carbon or of aluminum oxide.

Nanotubes (NT) are hollow entities which may consist of a single or of multiple walls and may exhibit open (*Fig. 1, q* and *s*) or closed ends (*Fig. 1, r* and *s*). In the latter case, the walls may be separated or a rolled sheet of material like the famous serpentine mineral (*Fig. 1, s* [7]).

2.3. *Two-Dimensional Nano Particles*

The class of 2D nano objects can only contain layer-like entities. Many related materials are applied in industrial processes, *e.g.*, graphite, molybdenum sulfide, pillared clays, and muskovite, just to mention a few. However, the sheet thicknesses of a few angstroms in these materials makes them belong much more to the molecular than to the nano regime. Again it is quite tricky and difficult to grow thicker layers or eventually such that different types of layers get together in a well-ordered form. Such quantum layers can be produced, *e.g.*, of semiconducting compounds, by molecular beam epitaxy, and their precise formation is essential, *e.g.*, for the construction of high-power semiconductor diodes. However, one should not only think of flat layers, because the planar arrangement is just a very specific case of curved topologies in general. We thus would like to discriminate the following 2D groups:

Planar layers (*Fig. 1, t*), **puckered layers** which extend in two dimensions (*Fig. 1, u*), and **hyperbolically curved layers** which extend in three dimensions (*Fig. 1, v*).

It is not surprising that tenside solutions allow for a consecutive generation of spheroid, tubular, layer-like arrangements (lamellar phases) which may be planar or curved, and finally curved layers which extend into 3D space. If the molecules in solution impose their shape or the shape of their aggregations onto another compound or material which forms from the same solution, then these molecules are struc-

ture-directing templates [8]. Quite recently, it has been shown that such tenside solution structures can mould novel forms of alumosilicates like the MCM41 and MCM48 materials with tube openings of more than 3 nm [9]. We have used a similar way in synthezising the vanadium oxide NTs which we will focus on in greater depth in the following.

3. Nanotubes

The serpentine or crysotile minerals are the best and longest known examples of all nanotubes. The compound $Mg_3(OH)_4[Si_2O_5]$ forms a double layer which consists of MgO_6 octahedra on the one side and SiO_4 tetrahedra on the other. As there is a small mismatch of the relative sizes of the different layers, the double layers roll up like a carpet [7][10][11].

Inorganic NTs and inorganic fullerene-related (IF) entities of early transition-metal disulfide compounds like VS_2, MoS_2, and WS_2 have been generated as well by *Tenne et al.* The syntheses are based on the preparation of corresponding compact oxide nano particles as precursors which are then reacted with H_2S to form the layered disulfides and finally the NTs and IFs. The latter ones are mainly wrapped around the solid cores of the residual oxide particles which act as inorganic templates [12]. Quite naturally, the quality of the NTs and IFs prepared by such a procedure is very much dependent on the definition of the precursor particles and on the actual growth processes, which
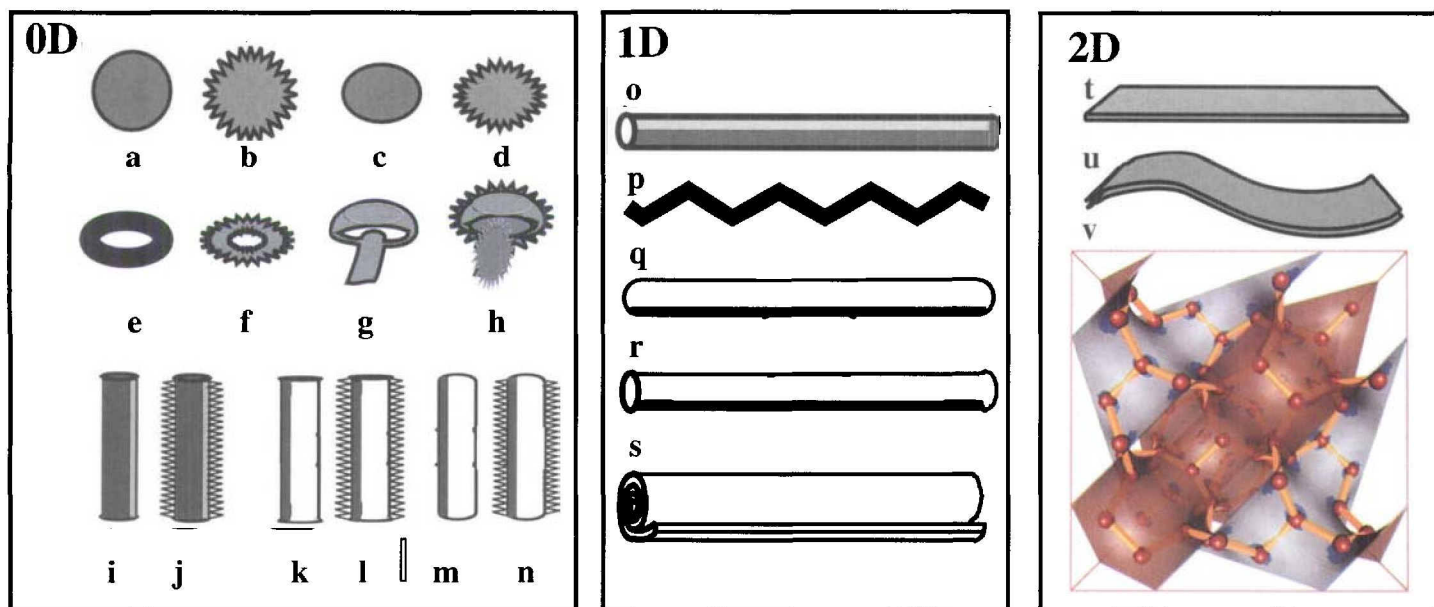

Fig. 1. *Schematic representation of nano particles grouped into* a–n) *zero-dimensional (0D)*, o–s) *one-dimensional (1D), and* t–v) *two-dimensional (2D) entities. a–d*) Compact and open dendrimer-like spheroids, *e), f*) tori, *i) j*) rods, *k), l*) open tubes, *m) n*) closed tubes, *o*) linear polymeric strand or rod, *p*) nonlinear polymer, *q*) closed tube, *r*) open tube, *s*) scroll, *t*) planar sheet, *u*) puckered layer, *v*) hyperbolic layer extending in 3D (the ball and stick model has been added to show how a descrete structure can follow such a hyperbolic topology).

are difficult to control [12–14]. Very small amounts of NT and IF materials have only been obtained in this way.

Another procedure makes use of carbon NTs (CNT) as outer templates. There are several publications on filling CNTs by different materials leading to formation of short solid rods [15–17]. Quite recently, the coating of CNTs by V_2O_5 was also reported resulting in the formation of a multilayered material [18][19]. Anodized aluminum metal develops layers of Al_2O_3 on the surface which shows nano pores of quite different sizes and packing densities [20], which can be used as outer templates for the formation of nanorod and nanotube arrays of different materials which may be deposited into the pores [20]. Even in the famous 'silica garden' experiment [21] nanofiber formation has just recently been observed [22].

Multiwalled carbon nanotubes (MWCNTs) are preferentially formed in carbon arc synthesis of fullerenes at the cathodic deposit as it had been first discovered by *Iijima* [23]. According to TEM investigations, MWCNTs are concentrical, helical tubes consisting of 1–50 bent graphite layers in a turbostratic arrangement with an outer diameter of 2–30 nm and lengths up to 1 µm. They are closed mostly on both sides, to a lesser extent only on one side, either with spherical, conical or polygonal caps. Most of the structural investigations of MWCNTs have been performed along longitudinal projection directions; *i.e.*, the tube axis is perpendicular to the electron beam. These investigations have shown that the carbon nanotubes consist of two sets of equally spaced parallel lattice fringes with d-spacings of 0.34 nm slightly greater than 0.334 nm for crystalline graphite, symmetrically arranged on opposite sides of the hollow core. From these investigations, a formation mechanism has been proposed [24] leading to a hollow concentric circular cylinder model (Russian doll model): starting from a fullerene dome at the cathodic surface, an initial tube is formed that grows parallel to the electrical field by adding successively C-atoms which form six-membered rings. This tube serves as a template for the second tube that grows epitactically around the first and so on (*cf. Fig. 2, a* and *b*). The incorporation of five-membered rings leads to the closure of the tubes.

However, this model can not explain the observations of several groups [25–27] that most of MWCNTs have asymmetrical structures, *i.e.*, usual lattice fringes with 0.34 nm spacings on one side and unusual lattice fringes with singular spac-
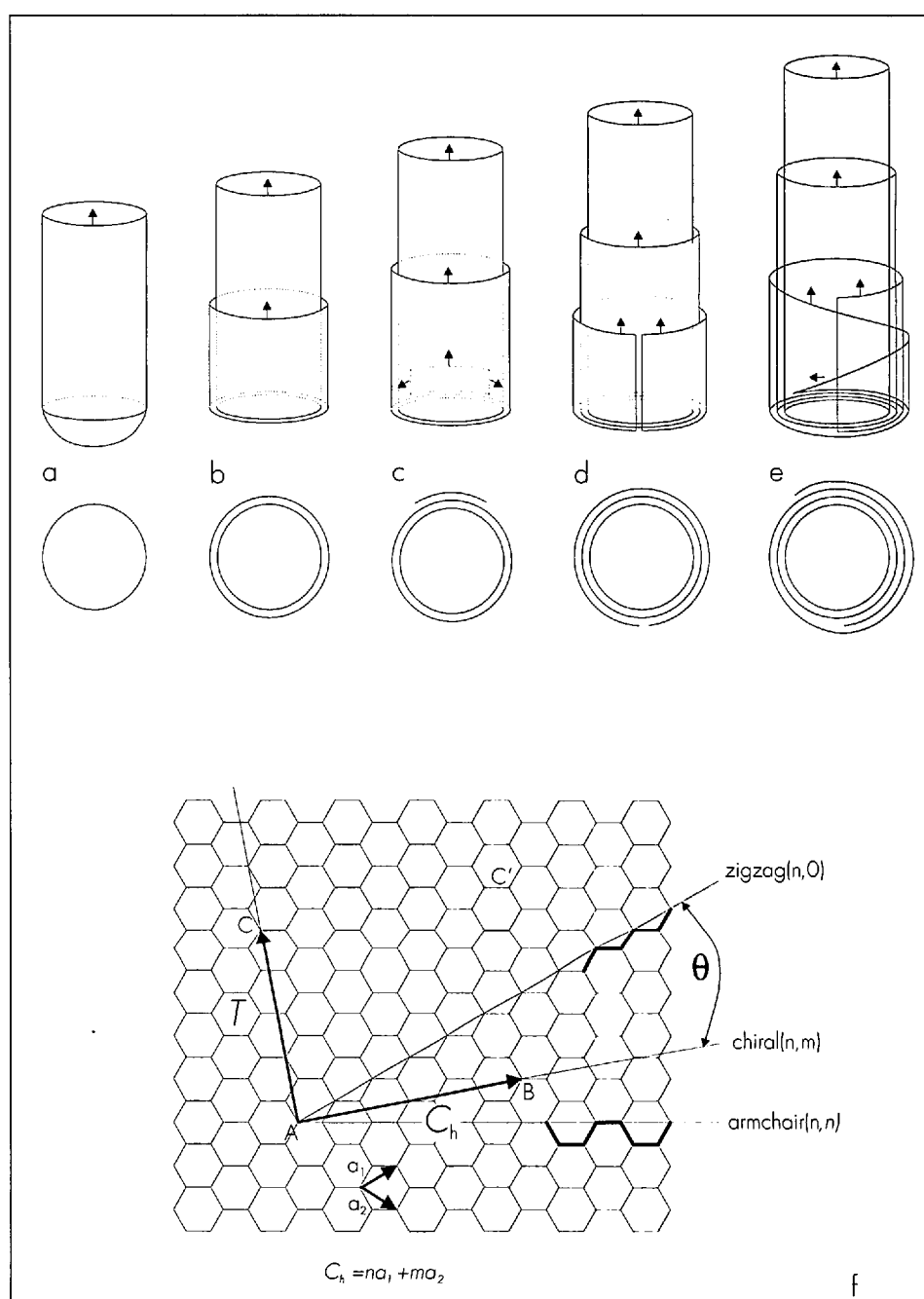

Fig. 2. *Proposed formation mechanism of multiwalled carbon nanotubes (MWCNTs).* The model describes the asymmetrical fringe patterns and deviations of fringe spacings frequently observed in TEM observations of the longitudinal structure of MWCNTs. Starting from a fullerene dome a tube starts to grow (*a*). The subsequent closed chiral sheet (*b*) serves as a template for the third (*c*) which does not close (*d*), because the induced helicity cannot be realized at this enhanced circumference. This gives rise to a dislocation, which finally leads to the formation of a scroll (*e*) and therefore to deviations of fringe spacings from the expected value. *f*) Construction principle of single-walled carbon nanotubes (SWNCTs). A graphene sheet is wrapped around a specific direction of the chiral vector C_h (defined by the unit vectors a_1 and a_2 and the chiral angle θ) leading to three different kinds of SWNCTs (zigzag (n,0), chiral (n,m), and armchair (n,n)) with a translational vector T parallel to the tube axis. Here, the orientation and length of C_h gives rise to a (4,2) chiral SWNCT.

ings larger than that. From these findings, another model has been developed which takes into account that the tubes might consist of scrolls rather than concentric cylinders. Simulations have shown that the scroll and cylinder images would be almost indistinguishable when viewed along a normal to the tube axis [28]. In this new model (*Fig. 2, a–e*), growth starts again from a fullerene dome of larger fullerenes, which are either chiral or achiral. A cylindrical tube is formed by preferential growth along the rim of this dome (*Fig. 2, a*). Even if the initial tube is achiral, a subsequent sheet generally has to become chiral when forming a cylinder (*Fig. 2, b*). The second sheet serves as a template for the third sheet which presum-

ably tends toward a graphitic stacking with the former, but a complete junction to a seamless cylinder is not possible because another chirality has to be realized due to the enhanced circumference (*Fig. 2, c*). This leads to a misfit along the meeting ledges giving rise to an edge-type *Frank* dislocation (*Fig. 2, d*). Therefore, this sheet now becomes a chiral scroll and its lateral growth leads to a number of sheets with the same chiral angle (*Fig. 2, e*). The tube, generated by this mechanism, would contain pairs of edge dislocations, which are roughly parallel to the tube axis and terminate successive scrolls.

Finally, HREM investigations of cross sections of carbon nanotubes [29] revealed MWCNTs to be polyhedral or elliptical along the tube axis with many defects in the microstructure, *e.g.*, edge-type dislocations and variable spacings between adjacent tube sheets. The application of both models (seamless cylinder and scroll) is suitable for the description of these observations.

Single-walled carbon nanotubes (SWCNTs) were first produced *via* co-vaporizing carbon and a transition metal (Fe, Co, Ni) in an arc generator [30][31]. The relatively low yields as well as the low purity of the samples regarding the large amorphous overcoating of the tubes in these initial experiments have been drastically improved using mixtures of transition metals [32][33]: especially Y in the presence of Co or Ni strongly favors the growth of SWCNTs leading to yields in the range of 70–90%. Alternatively, pure SWCNTs can be produced in high yields (50–70%) by laser vaporization of transition metal (metal-mixture)/graphite composite rods in the condensing vapor in a heated flow tube [34][35]. The extreme uniformity of the diameters of these SWCNTs (1.4 Å) leads to a self-organization into crystalline 'ropes' or bundles consisting of 20 [33] or 100–500 [35] SWCNTs in a two-dimensional triangular lattice with $a = 17$ Å in the latter case. A four-probe resistivity measurement revealed that the SWCNTs ropes are metallic.

From these observations, a 'scooter' mechanism has been hypothesized for the preferential formation of apparently one type of SWCNT: A metal atom (Ni) scoots along the rim of an initial fullerene dome preventing the formation of any energetically unfavorable carbon structure (*e.g.*, incorporation of five-membered rings) by catalyzing the rearrangement of C-atoms during growth. If the number of C-atoms is within a specific critical size range, the most favored (10,10) armchair configura-

tion of the resulting metallic SWCNT is realized as observed in these experiments.

Three different kinds of SWCNTs can be theoretically constructed by rolling a planar graphene sheet around a vector C_h of a certain direction on the sheet to form an open cylinder and close them with fullerene domes (*Fig. 3*) [36][37]. The vector $C_h = na_1 + ma_2$, which is perpendicular to the tube axis, is defined by different combinations of the unit vectors a_1 and a_2 on the honeycomb lattice and the chiral angle θ with respect to the zigzag axis: *a)* $\theta = 30°$ yields an (n,n)-'armchair' tube, *b)* $\theta = 0°$ an (n,0)-'zigzag', and *c)* a general direction between 0 and 30° an (n,m)-'chiral' tube. Theoretical calculations [38][39] revealed that the physical properties of the nanotubes strongly depend on diameter and helicity, and, therefore, symmetry dictates the physical properties: (n,n)-armchair tubes have band crossings at the *Fermi* level and therefore are expected to be metallic as well as (n,0)-zigzag or (n,m)-chiral tubes with n–m = 3 l (l is an integer), whereas in the case of n–m ≠ 3 l semiconducting behavior is predicted with a band gap of *ca.* 0.5 eV. Quite recently, these predictions, especially those concerning the strong one-dimensional nature of conduction, have been confirmed from atomically resolved STM images and STS of individual SWCNTs [40][41].

Vanadium-oxide nanotubes (VO$_x$-NTs) were obtained as main product *via* a sol-gel reaction from vanadium-alkoxide precursors and primary amines $(C_nH_{2n+1}NH_2, n = 4–22)$ which act as templates [42][43]. The first step of the synthesis is the formation of a lamellar structured composite of surfactant and vanadium oxide which is obtained by hydrolysis of an alcoholic solution of a vanadium-triisopropoxide amine adduct. Hydrothermal treatment of this composite at 180° leads to the formation of isolated VO$_x$-NTs after one week. The nominal composition is $VO_{2.4}(C_{16}H_{33}NH_2)_{0.34}$ when hexadecylamine is used as structure-directing agent.

Depending on the synthesis conditions, *e.g.*, concentration or types of template, VO$_x$-NTs appear as either open or closed multiwalled tubes (*Fig. 3, a*). The walls consist of 2–20 sheets with outer diameters ranging from 15 to 100 nm. The tube openings vary between 5 and 50 nm, and maximum lengths up to 15 μm are observed. VO$_x$-NTs are frequently grown together in the form of bundles. In the electron diffraction patterns, the average layer thickness of the walls present in the tubes gives rise to a corresponding row of sharp reflections with narrow distances

close to the center of reciprocal space. This fact indicates that the wall layers are indeed well-ordered and oriented in a parallel manner in the observed area. However, further *Bragg* reflections are present, which are arranged on a square with an edge length of *ca.* 0.62 nm and which are caused by the structure within the layers. Remarkably, these reflections appear on the same sites in all NT samples, while the distance between the reflections in the row significantly shifts with the layer thickness which varies with the template. This row of reflections is rotated by 45° in respect to the square of reflections, indicating a well-defined orientation relationship between layer structure and the walls. Due to the bending of the layers as well as to defects of the nanotubes, the square of reflections is blurred in most cases. It should be noted that the electron diffraction pattern reveals more structural information than HRTEM images: the square structure of the layers is mostly not recognizable since this part of the structure is destroyed by the intense electron beam which is necessary to record the HRTEM images. Only the shell structure withstands this treatment. In addition, also the row of reflections disappeared quite often in the beam, indicating that the shells have become less ordered.

A good correlation between the data obtained from diffraction methods and from TEM is gained regarding the reflections caused by the structure within the layers. The square arrangement of spots in the electron diffraction patterns as well as the set of four less intense peaks at smaller d-values in the X-ray powder diffractogram can be indexed on the basis of a two-dimensional square lattice with $a = 0.62$ nm. On the other hand, there is a certain discrepancy between the data obtained by the two methods: the peak with the highest intensity in the 001 series of reflections in the X-ray powder patterns appears at d-values between 1.5 and 3 nm and, thus, corresponds to the distance of the shell layers. This value is sometimes 6–8 Å larger than the one determined by electron diffraction or from HRTEM images. This might be due to a certain rearrangement of the template molecules between the sheets under the influence of the electron beam giving rise to smaller sheet distances. This phenomenon, which could not be induced thermally to that extent, can be sufficiently explained with a flexible structural model proposed below.

As it is already apparent from TEM observations of the longitudinal structure, the diameters of the nanotubes vary in a wide range (approximately between 30

and 100 nm) owing to different numbers of the layers. The shell structure of the nanotubes is directly visible in the cross-sectional HRTEM images (*Fig. 3, b–f*). It is obvious, that most nanotubes are not rotationally symmetric; depressions and holes appear frequently. Furthermore, they rather form rolls of layers than concentric shells (*Fig. 3, b*). The contrast of the nanotube walls is often blurred at a distinct site; this fact impedes an unambiguous discrimination between a cylindric tube structure and rolled layers. A clear concentric tubular arrangement is only found in tubes consisting of four or fewer sheets, which are rarely observed (< 1%). Sometimes, scrolls with a seam on one side have been observed. Moreover, sheets are only partially closed or irregularly arranged appearing as open half cycles (*Fig. 3, e* and *f*).

In cross-sectional HRTEM images as well as in the longitudinal projection direction, a weak contrast between the sheets has been observed which can be attributed to a monolayer of protonated amine molecules in a paraffin-like arrangement. Such monolayers were frequently observed in alkylamin-intercalated sheet structures of a large variety of substances [44]. This assumption of a monolayered structure is supported by the following experimental facts: *1*) The template molecules can be substituted either by a cation exchange against, *e.g.* , alkali cations, or by a proton exchange with neutral amines or diamines; *2*) The exchange reaction with diamines leads to the formation of rather short tubes (1–2 μm) with a well-ordered sheet structure and uniform distances throughout the tube length. The inner diameters of these tubes have increased in the average by *ca.* 40%. In the cross section, these tubes appear either as closed scrolls or, frequently, as open half cycles with a well-ordered sheet arrangement and without those holes which are often observed in VO$_x$-NTs with monoamines as templates (*Fig. 3, d*). Apparently, an entropically driven exchange reaction of two monoamine molecules with one diamine molecule took place, which leads to a stiffening of the sheet structure and, therefore, to higher structural order.

The scroll structure in conjunction with the flexible paraffin-like monolayers of the template molecules between the sheets is an arrangement of extraordinary flexibility that is capable of compensating any strain imposed on the tubes very efficiently by realization of a large variety of sheet distances. Different forms of strain can be encountered: *1*) The enormous reduction of the sheet distance from 3 to 0.86 nm
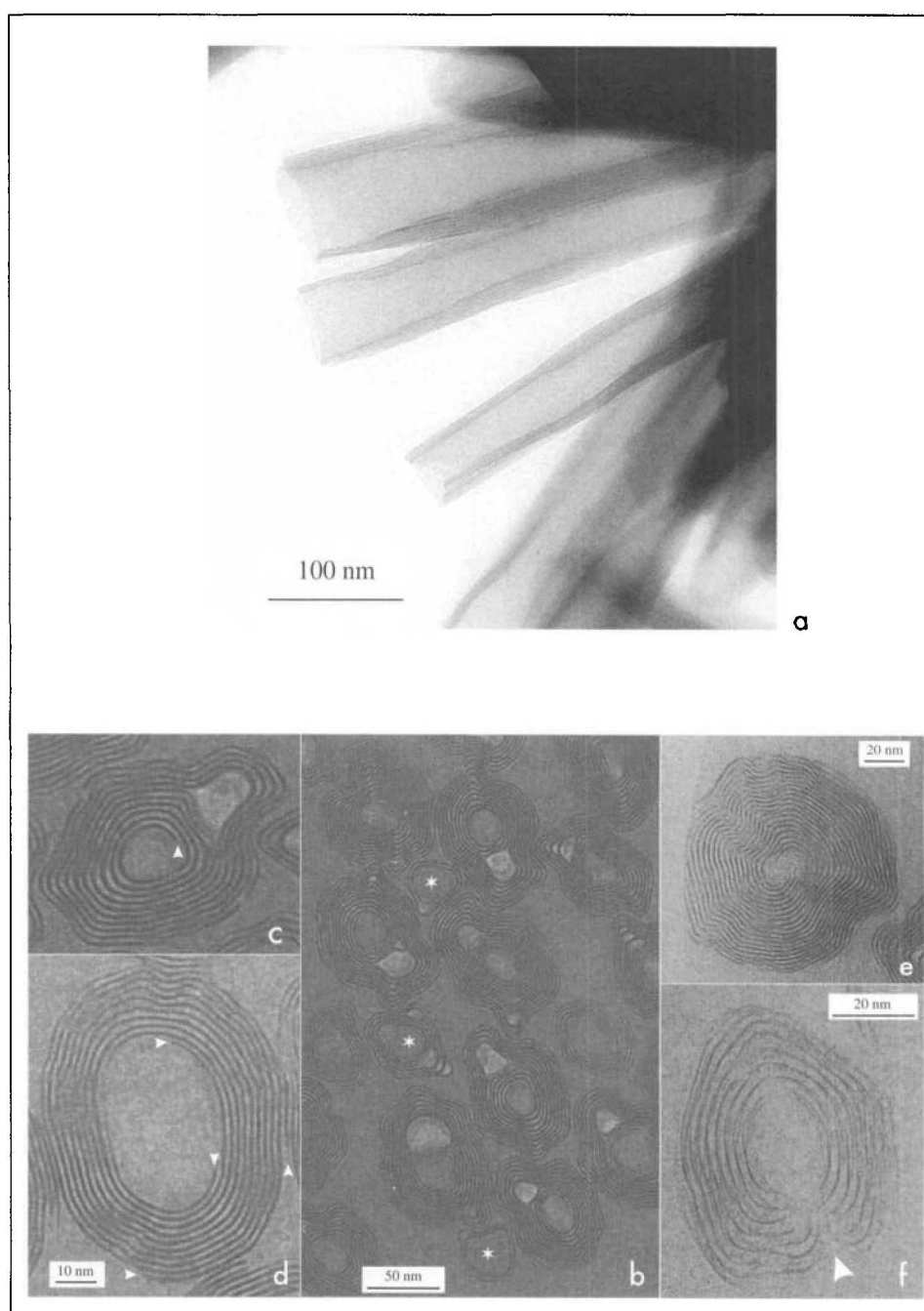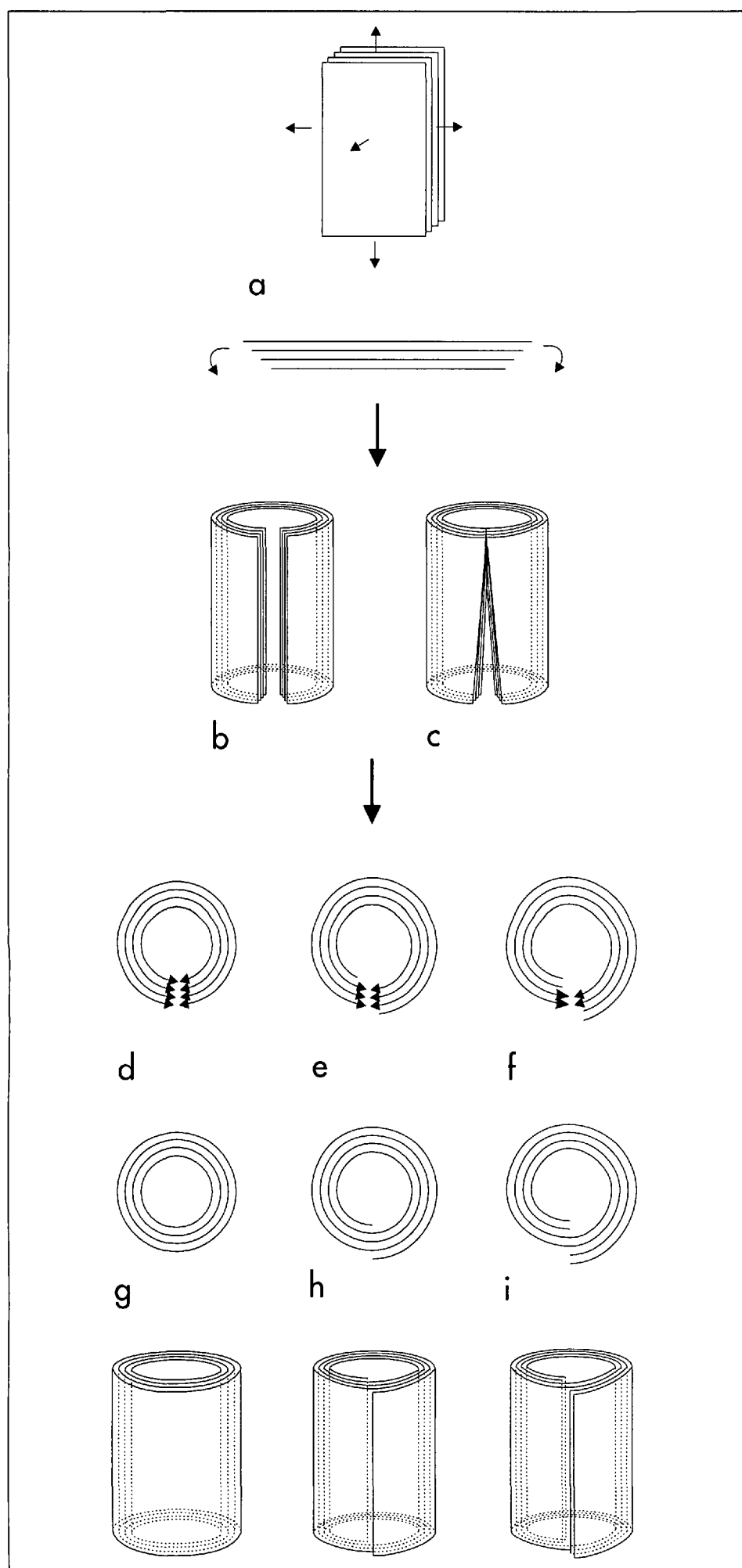

Fig. 3. a) *Typical TEM image of vanadium-oxide nanotubes (VO$_x$-NTs) with hexadecylamine (HDA) as template obtained after hydrothermal synthesis.* b) *TEM image of cross sections of HDA-VO$_x$-NTs: concentrical tube structures* (marked by asterisks) *are present besides single- and double-layer scrolls.* c) *Higher magnification of a single-layer scroll* (the lower edge of the image corresponds to 100 nm): the starting point of the scrolled sheet in the center of the tube is marked by an arrow. Holes within the tubes are frequently observed in cross sections of monoamine-VO$_x$-NTs. d) *Cross section of a double-layer scroll* (arrows) *obtained by an exchange reaction of HDA-VO$_x$-NTs with dodecyldiamine.* The well-ordered sheet structure as well as the enhanced inner diameter compared to *c*) is striking. e) *A five-layer undecylamine-VO$_x$-NT built up of twenty sheets:* variations in the fringe spacings lead to a disordered sheet structure. f) *An incompletely closed undecylamine-VO$_x$-NT.*

caused by cation exchange of protonated hexadecylamine with ammonium cations under preservation of the tube morphology can only be rationalized with the scroll structure. *2*) Strain, which was imposed by external pressure during embedding the tubes in a polymer matrix for the cross-sectional analysis, partially leads to a deformation of the tubes, *i.e.*, a variety of sheet distances in one tube can only be

realized by the flexibility of the template arrangement. The latter might also be responsible for the above-mentioned discrepancy between the sheet distances determined by X-ray powder diffraction and by HREM investigations.

To explain these observations, the following model is proposed (*Fig. 4, a–f*): Starting from a lamellar arrangement of vanadium-oxide sheets separated by a par-

affin-like arrangement of template molecules (*Fig. 4, a*), the sheets start to bent (*Fig. 4, b*) and close after exceeding a certain sheet width realizing the circumference of the scroll or tube determined by the length of the alkylamines. In such a process, different tube structures may form: *1*) A concentric tubular arrangement where the sheet ledges meet in the right way, which is only likely to be realized if a relatively small number of sheets is present (*Fig. 4, d*). 2) A dislocation of one-sheet gives rise to a one sheet scroll after closure (*Fig. 4, e*). 3) A dislocation of two sheets leads to the formation of a double-layer scroll (*Fig. 4, f*). The probability of sheet dislocations is higher if a larger number of sheets is involved. Different sheet widths in the lamellar structure lead either to incomplete closure or widening of the sheet distances (holes and depressions in the tubes and scrolls (*cf. Fig. 3, b*). The structure of such scrolls can be described by the 'paper-mache' model proposed for MWCNTs [28]. A 'zip'-like rather than a 'scrolling of a carpet'-mechanism (*Fig. 4, c*) can be assumed for the curling and closure of the sheets, exceeding gradually over the whole tube length. This may give rise to various kinds of dislocations along the tube which is expressed in different fringe spaces and nonsymmetrical fringe patterns in the longitudinal projection direction of VO_x-NTs.

The driving force for the bending of the sheets is not yet clear, but there are different possibilities at hand: *1*) As proposed by *A. Müller et al.* [45][46], the introduction of mixed valency into a vanadium- or molybdenum-oxide structure may induce the necessary curvature. In this case, the extent of curvature should be a selective function of the redox state of the transition metal. *2*) The anisotropic attachment of a few template molecules to a small oligooxometallate group may curve the metallate moiety [47]. However, this

Fig. 4. *Proposed formation mechanism of VO_x-NTs.* Starting from a lamellar, anisotropically extended sheet structure composed of vanadium-oxide sheets separated by double layers of protonated mono-amine molecules, the sheets starts to bent (*a, b*). The sheet ledges either close perfectly (*d*) to a concentrical set of cylinders (*g*), or miss each other in that way that dislocations of either one (*e*) or two sheets (*f*) occur which give rise to single- (*h*) or double-layer scroll (*i*). A possible 'zip'-like closure mechanism is illustrated in *c*)

must be a very favorable pathway for this reaction taking into account the outstanding yield of VO_x-NTs in our synthesis. 3) The dangling bonds at the border of a narrow sheet can be saturated forming NTs *via* a zip mechanism, as already mentioned, or directly during the growth process of the sheet. It seems quite reasonable that, under well-chosen conditions, most layer structures should be transformable into nanotubes.

However, the question where the narrow sheets arise from must find another answer that may be due to a prestructuring process. It has been observed many times that V_2O_5 gels adopt fibrillar or ribbon-like structures [48–50], indicating that the growth processes of the individual layers are highly anisotropic.

4. Possible Applications

There are many hypothetical and but only some really tested applications of nanotubes, however, all of which appear to be quite fascinating. An obvious application is to use NTs as storage devices. As already mentioned, incorporation of different materials into carbon NTs has been shown. More attracting, however, are reports of hydrogen [51] and lithium uptake [52][53] giving rise to extremely good storage densities. The electronic transport in CNTs has been measured and quantisized one-dimensional conduction characteristics have been found [40][41][54][55]. In a recent theoretical work, CNTs are proposed as long ballistic conductors [56]. There are several proposals for using CNTs as high-strength-elastic nano springs and levers [57–59]. Application as tips for scanning microsopy has been proved to be very powerful (*cf. Fig. 5, e*), but the tip preparation is still very difficult [60][61]. A further step is the functionalization of the tip of the CNTs by attaching molecules with functional groups making it a selective nano probe in chemistry and biology [62].

As the anisotropy of NTs is so large and their form is quite special they allow for principle functionalization at three distinct regions: the inner surface, the outer wall, and the tube ends, which may be distinct enough to be selectively contacted or functionalized. Multiple walled NTs offer under certain circumstances for an introduction of guests in between the walls. This gives rise to numerous speculations about possible nano devices (*cf. Fig. 5, a–d*), like nano sensors, nano transistors [63–66], nano electrodes, and nano reaction vessels [67–70], which may, *e.g.*, limit the
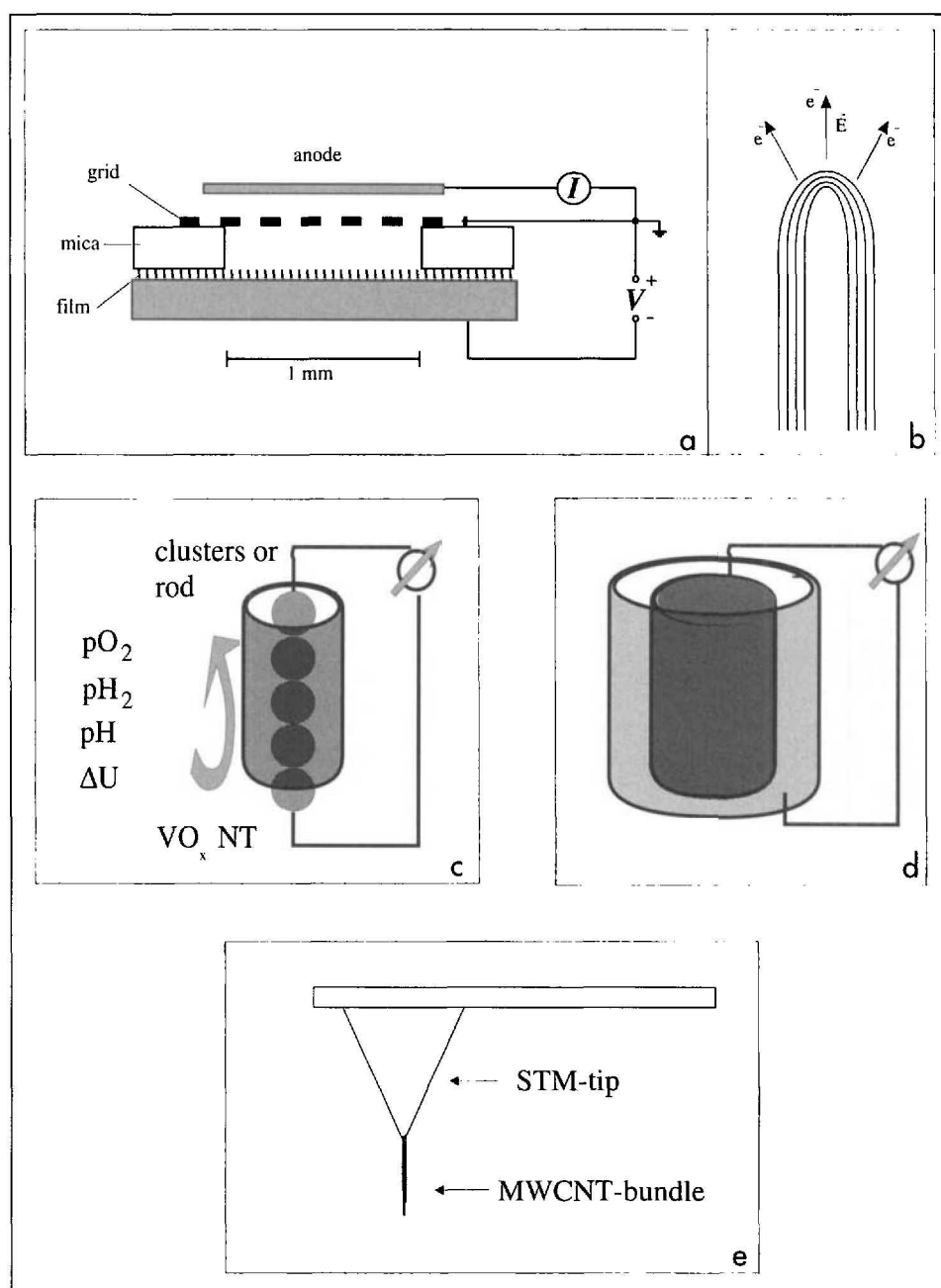
Fig. 5. a) *Model of a field emission device constructed from a film of aligned MWCNTs.* b) *Schematic representation of the electrical field at the tip surface of a closed MWCNT.* c) *Schematic model of a nano sensor built of a nanotube and self-assembled conducting entities inside the tube.* In case of the VO_x NTs the walls should change their chemical potential with respect to changes of pH, pH_2, pO_2, or an outer electrical field. d) *Schematic representation of a nano capacitor made of two different NTs.* e) *Schematic illustration of a bundle of MWCNTs attached to the probe tip of a STM.* The bundle tampers to a single CNT at the lower end.

polymer length during a polymerization process inside an NT. Surely, there are still many difficult problems to solve towards such devices, but it seems that we are close to finding feasable roads and – do we really have other alternatives?

We are very much indepted to Dr. *Frank Krumeich* for the transmission electron micrographs and to the *Jubiläumsfond of ETH-Zürich* for the generous support under the TEMA project.

[1] R.S. Berry, *Nature (London)* **1998**, *393*, 212.

[2] M. Schmidt, R. Kusche, B. von Isendorff, H. Haberland, *Nature (London)* **1998**, *393*, 238.

[3] M.S. Dresselhaus, G. Dresselhaus, P.C. Eklund, 'Science of Fullerenes and Carbon Nanotubes', Academic Press, New York, 1996.

[4] A. Müller, E. Krickemeyer, J. Meyer, H. Bögge, F. Peters, W. Plass, E. Diemann, S. Dillinger, F. Nonnenbruch, M. Randerath, C. Menke, *Angew. Chem.* **1995**, *107*, 2293; *ibid., Int. Ed. Engl.* **1995**, *34*, 2122.

[5] A. Müller, E. Krickemeyer, H. Bögge, M. Schmidtmann, C. Beugeholt, P. Körgeler, C. Lu, *Angew. Chem.* **1998**, *110*, 1278; *ibid., Int. Ed. Engl.* **1998**, *37*, 1220.

[6] S.I. Stupp, V. LeBonheur, K. Walker, L.S. Li, K.E. Huggins, M. Keser, A. Amstutz, *Science* **1997**, *276*, 384.

[7] E.J.W. Whittaker, *Acta Crystallogr.* **1956**, *9*, 855.

[8] A. Müller, H. Reuter, S. Dillinger, *Angew. Chem.* **1995**, *107*, 2505; *ibid., Int. Ed. Engl.* **1995**, *34*, 2311.

[9] J.S. Beck, J.C. Vartuli, W.J. Roth, M.E. Leonowicz, C.T. Kresge, K.D. Schmidt, C.T.-W. Chu, D.H. Olson, E.W. Sheppard, S.B. McCullen, J.B. Higgins, J.C. Schlenker, *J. Am. Chem. Soc.* **1992**, *114*, 10834.

[10] K. Yada, *Acta Crystallogr., Sect. A* **1971**, *27*, 659.

[11] F. Liebau, 'Structural Chemistry of Silicates', Springer-Verlag, Berlin, 1985.

[12] R. Tenne, L. Margulis, Y. Feldmann, M. Homyonfer, *Mat. Res. Soc. Symp. Proc.* **1995**, *359*, 111.

[13] M. Homyonfer, B. Alperson, Y. Rosenberg, L. Sapir, S.R. Cohen, G. Hodes, R. Tenne, *J. Am. Chem. Soc.* **1997**, *119*, 2693.

[14] R. Tenne, *Endeavour* **1996**, *20*, 97.

[15] P.M. Alayan, S. Iijima, *Nature (London)* **1993**, *381*, 333.

[16] S.C. Tsang, Y.K. Chen, P.J.F. Harris, M.L.H. Green, *Nature (London)* **1994**, *372*, 159.

[17] C. Guerret-Piecourt, Y. Le Bouar, A. Loiseau, H. Pascard, *Nature (London)* **1994**, *372*, 761.

[18] P.M. Alayan, O. Stephan, Ph. Redlich, C. Colliex, *Nature (London)* **1995**, *375*, 564.

[19] B.C. Satiskumar, A. Govindarja, E.M. Vogl, L. Basumallick, C.N.R. Rao, *J. Mater. Res.* **1997**, *12*, 604.

[20] J.C. Hultgren, C.R. Martin, *J. Mater. Chem.* **1997**, *7*, 1075.

[21] W.J. Clunis Ross, *Proc. R. Soc. NS Wales* **1910**, *44*, 583.

[22] C. Collins, W. Hou, A.L. Mackay, J. Klinowski, *Chem. Phys. Lett.* **1998**, *286*, 88.

[23] S. Iijima, *Nature (London)* **1991**, *354*, 56.

[24] X.F. Zhang, X.B. Zhang, G. van Tendeloo, S. Amelinckx, M. op de Beeck, *J. Cryst. Growth* **1993**, *130*, 368.

[25] M. Liu, J.M. Cowley, *Carbon* **1994**, *32*, 393.

[26] S. Amelinckx, D. Bemaerts, S.B. Zhang, G. van Tendeloo, J. van Landuyt, *Science* **1995**, *267*, 1334.

[27] N. Wang, K.K. Fung, W. Lu, S. Yang, *Chem. Phys. Lett.* **1994**, *229*, 587.

[28] O. Zhou, R.M. Fleming, D.W. Murphy, C.H. Chen, R.C. Haddon, A.P. Rainirez, S.H. Glarum, *Science* **1994**, *263*, 1744.

[29] S.Q. Feng, D.P. Yu, G. Hu, X.F. Zhang, Z. Zhang, *J. Phys. Chem. Solids* **1997**, *58*, 1887.

[30] S. Iijima, T. Ichihashi, *Nature (London)* **1993**, *363*, 603.

[31] D.S. Bethune, C.H. Kiang, M.S. de Vries, G. Gorman, R. Savoy, J. Vazquez, R. Beyers, *Nature (London)* **1993**, *363*, 605.

[32] J.M. Lambert, P.M. Ajayan, P. Bernier, J.M. Planeix, V. Brontons, B. Coq, J. Castaing, *Chem. Phys. Lett.* **1994**, *226*, 364.

[33] C. Journet, W.K. Maser, P. Bernier, A. Loiseau, M. Lamy de la Chapelle, S. Lefrant, P. Deniard, R. Lee, J.E. Fischer, *Nature (London)* **1997**, *388*, 756.

[34] T. Guo, P. Nikolaev, A. Thess, D.T. Colbert, R.E. Smalley, *Chem. Phys. Lett.* **1995**, *243*, 49.

[35] A. Thess, R. Lee, P. Nikolaev, H. Dai, P. Petit, J. Robert, C. Xu, Y.H. Lee, S.G. Kim, A.G. Rinzler, D.T. Colbert, G.E. Scuseria, D. Tomanek, J.E. Fischer, R.E. Smalley, *Science* **1996**, *273*, 483.

[36] M.S. Dresselhaus, G. Dresselhaus, R. Saito, *Phys. Rev. B* **1992**, *45*, 6234.

[37] M.S. Dresselhaus, G. Dresselhaus, R. Saito, *Carbon* **1995**, *33*, 883.

[38] R. Saito, M. Fujita, G. Dresselhaus, M.S. Dresselhaus, *Phys. Rev. B* **1992**, *46*, 1804.

[39] R. Saito, G. Dresselhaus, M.S. Dresselhaus, *Chem. Phys. Lett.* **1992**, *195*, 537.

[40] J.W. Wildöer, L.C. Venema, A.G. Rinzler, R.E. Smalley, C. Dekker, *Nature (London)* **1998**, *391*, 59.

[41] T.W. Odom, J.L. Huang, P. Kim, C.M. Lieber, *Nature (London)* **1998**, *391*, 62.

[42] R. Nesper, M.E. Spahr, M. Niederberger, P. Bitterli, Int. Pat. Appl. PCT/CH97/00470, Bundesamt für Geistiges Eigentum, Bern, 1997.

[43] M.E. Spahr, P. Bitterli, R. Nesper, M. Müller, F. Krumeich, H.U. Nissen, *Angew. Chem.* **1998**, *110*, 1339; *ibid., Int. Ed. Engl.* **1998**, *37*, 1263

[44] G. Lagaly, *Solid State Ionics* **1986**, *22*, 43.

[45] A. Müller, J. Meyer, E. Krickemeyer, E. Diemann, *Angew. Chem.* **1996**, *108*, 1296; *ibid., Int. Ed. Engl.* **1996**, *35*, 1206.

[46] A. Müller, M. Penk, R. Rohlfing, E. Krickemeyer, J. Döring, *Angew. Chem.* **1990**, *102*, 927; *ibid., Int. Ed. Engl.* **1990**, *29*, 926.

[47] M. Brändle, R. Nesper, preliminary results of molecular dynamics studies, unpublished.

[48] J. Livage, *Chem. Mater.* **1991**, *3*, 578.

[49] J.J. Legendre, J. Livage, *J. Colloid Interface Sci.* **1983**, *94*, 75.

[50] P. Davidson, C. Bourgeaux, L. Schoutteten, P. Sergot, C. Williams, J. Livage, *J. Phys. (Paris) II* **1995**, *5*, 1577.

[51] A.C. Dillon, K.M. Jones, T.A. Bekkedahl, C.H. Kiang, D.S. Bethune, M.J. Heben, *Nature (London)* **1997**, *386*, 377.

[52] G. Che, B.B. Lakshmi, E.R. Fisher, C.R. Martin, *Nature (London)* **1998**, *393*, 346.

[53] M. Freemantle, *Chem. Eng. News* **1996**, *74*, 62.

[54] M. Bockrath, D.H. Cobden, P.L. McEuen, N.G. Chopra, A. Zettl, A. Thess, R.E. Smalley, *Science* **1997**, *275*, 1922.

[55] S.J. Tans, M.H. Devoret, H. Dai, A. Thess, R.E. Smalley, L.J. Geerlings, C. Dekker, *Nature (London)* **1997**, *386*, 474.

[56] P. Delaney, H.J. Choi, J. Ihm, S.G. Louie, M.L. Cohen, *Nature (London)* **1998**, *391*, 466.

[57] E.W. Wong, P.E. Sheehan, C.M. Lieber, *Science* **1997**, *277*, 1971.

[58] R.S. Ruoff, D.C. Lorents, R. Laduca, S. Awadalla, S. Weathersby, K. Parvin, S. Subramoney, in Proceedings of the Symposium on Recent Avances in the Chemistry and Fullerenes and Related Materials, 1995, Electrochemical Society, New Jersey, pp. 557–569.

[59] T. Hertel, R. Martel, P. Avouris, *J. Phys. Chem. B* **1998**, *102*, 910.

[60] H. Dai, J.H. Hafner, A.G. Rinzler, D.T. Colbert, R.E. Smalley, *Nature (London)* **1996**, *384*, 147.

[61] S.S. Wong, J.D. Harper, P.T. Lansbury, C.M. Lieber, *J. Am. Chem. Soc.* **1998**, *120*, 603.

[62] S.S. Wong, E. Joselevich, A.T. Woolley, C.L. Cheung, C.M. Lieber, *Nature (London)* **1998**, *394*, 52.

[63] L. Kouwenhoven, *Science* **1997**, *275*, 1896.

[64] S. Saito, *Science* **1997**, *278*, 77.

[65] P.L. McEuen, *Nature (London)* **1998**, *393*, 15.

[66] S.J. Tans, A.R.M. Verschueren, C. Dekker, *Nature (London)* **1998**, *393*, 49.

[67] D. Ugarte, A. Châtelain, W.A. de Heer, *Science* **1996**, *274*, 1897.

[68] J. Sloan, J. Hammer, M. Zwiefka-Sibley, M.L.H. Green, *Chem. Commun.* **1998**, 347.

[69] J.J. Davis, M.L.H. Green, H.A.O. Hill, Y.C. Leung, P.J. Sadler, J. Sloan, A.V. Xavier, S.C. Tsang, *Inorg. Chim. Acta* **1998**, *272*, 261.

[70] Z. Guo, P.J. Sadler, S.C. Tsang, *Adv. Mater.* **1998**, *10*, 701.